RESEARCH | Article in Press

Microhybridization enhances intestinal microbiota and glycometabolic regulation in natural gynogenic blunt snout bream derived from the blunt snout bream (*Megalobrama amblycephala*, ♀) × Chinese perch (*Siniperca chuatsi*, ♂)

Yuhuan Wei · Rui Dai · Mingguang Hu · Shijia Lei · Jie Tang · Siyao Weng · Ya Zeng · Yue Ding · Qinbo Qin · Ting Yi · Min Wang · Min Tao · Chun Zhang · Ping Wu · Qizhi Liu · Shaojun Liu

Received: 13 April 2026 / Accepted: 10 September 2026
© The Author(s) 2026

Abstract

Background Gut microbiota plays critical roles in host nutrition and metabolism, but research on the intestinal nutrition and gut microbiota of gynogenetic offspring, especially from omnivorous and carnivorous crosses, remains scarce.

Methods Intestinal tissues were collected from natural gynogenetic blunt snout bream (GBSB) and its parents (*Megalobrama amblycephala* ♀ and *Siniperca chuatsi* ♂) for metagenomic sequencing, histological examination, enzyme activity assay, and quantitative gene expression quantification. Pearson correlation analysis was also performed to determine the correlations between microbial functional abundance and metabolic gene expression.

Results Our study found that the intestinal of GBSB exhibited higher antioxidant (catalase, reduced glutathione) and digestive enzyme (alkaline xylanase, acid phosphatase, lipase) activities than normal blunt snout bream (BSB). Metabolically, the expression levels of glycolysis-related genes (*GADPH*, *Idha*) were downregulated in GBSB, whereas those of pentose phosphate pathway genes (*Pgd*, *Taldo1*) were upregulated. The gut microbiota in GBSB closely resembled that in the maternal line, sharing Bacillus as a dominant genus, although shifts occurred within the Bacteroidota and Pseudomonadota phyla. Correlation analysis suggested that heterologous sperm induction altered host gene expression, which drove gut microbiota restructuring through host-microbiota interactions in sugar metabolism.

Conclusions In general, microhybridization improved the digestion performance of GBSB, and its glucose metabolism pathways such as glycolysis, pentose phosphate pathway and tricarboxylic acid cycle were regulated to a certain extent compared with the maternal parent. These host metabolism-microbiota dynamics are crucial for optimizing feeding strategies and health management in novel gynogenetic fish breeds.

This Article in Press is shared early to give you faster access to new research. It is citable and carries a permanent DOI. The final edited version will replace it automatically.

Yuhuan Wei and Rui Dai contributed equally to this work.

https://doi.org/10.1186/s12864-026-13359-6

Published online: 16 September 2026

Keywords Gynogenesis · Microhybridization · Gut microbiota · Host-microbe interactions · Glucose metabolism

Abbreviations

Aco2	Aconitase 2
ACP	Acid phosphatase
ACX	Acid xylanase
AMS	α-Amylase
BAX	Alkaline xylanase
BSB	Blunt snout bream
CAT	Catalase
CL	Cellulase
CP	Chinese perch
Cs	Citrate synthase
CuZn-SOD	Zinc–copper superoxide dismutase
GAPDH	Glyceraldehyde-3-phosphate dehydrogenase
GBSB	Gynogenic blunt snout bream
GSH	Reduced glutathione
Idha	Isocitrate dehydrogenase alpha
LPS	Lipase
MDA	Malondialdehyde
Mdh2	Malate dehydrogenase 2
Ogdh	Oxoglutarate dehydrogenase
OTUs	Operational taxonomic units
PBS	Phosphate buffered saline
Pgd	Phosphogluconate dehydrogenase
pgk1	Phosphoglycerate kinase 1
pgls	6-Phosphogluconolactonase
PPP	Pentose phosphate pathway
Prkaa	Protein kinase, AMP-activated, alpha subunit
RGL	Relative gut length
SCFA	Short-chain fatty acids
sdha	Succinate dehydrogenase complex flavoprotein subunit a
sdhc	Succinate dehydrogenase complex subunit c
SOD	Superoxide dismutase
suclg1	Succinate-CoA ligase GDP-forming subunit beta
Taldo1	Transaldolase 1
TCA	Tricarboxylic acid
TEM	Transmission electron microscopy
Tkt	Transketolase

Introduction

The composition of intestinal microorganisms in fish is determined by their physiological structure and food consumption (herbivory and carnivory). However, the gut of herbivorous fish is much longer than that of carnivorous fish. To adapt to longer digestion, the submucosa of herbivorous fish may be more developed, and the muscularis

more slender. For carnivorous fish to adapt to rapid digestion, their muscularis may be relatively short and thick [1]. Due to the genetic effect of chromosome assembly, the gut length in the offspring of hybrid carnivorous and herbivorous fish is between that of the parents, as verified in reciprocal hybrids of blunt snout bream (BSB) and Topmouth Culter (TC) [2].

The dominant gut microorganisms in fish are usually bacteria [3], which are mainly composed of aerobic and facultative anaerobic bacteria. The intestinal microflora diversity in fish is significantly affected by feeding habits [1, 4], with omnivorous fish having the greatest diversity of bacterial species, followed by herbivorous fish, and carnivorous fish [5]. Long-term dietary differentiation drives the formation of functionally differentiated intestinal microbial communities in fish with different feeding preferences [6]. Carnivorous fish, adapted to a high-protein and high-fat diet, harbor gut microbiota dominated by the phyla Proteobacteria and Firmicutes, enriched with taxa such as *Aeromonas*, *Vibrio*, and *Photobacterium*, which efficiently degrade proteins and lipids [7]. By contrast, herbivorous fish face the challenge of degrading cellulose and hemicellulose in plant cell walls [8]. Their microbiota is characterized by a high abundance of Bacteroidetes and polysaccharide-degrading members of Firmicutes [9]. In offspring obtained by distant hybridization of fish with different dietary habits, their microbial structure (composition and abundance) lies between those of the parents [2] because of subgenome dominance [10]. Nevertheless, gynogenetic progeny exhibit obviously different intestinal microbiota from their maternal parents [11]. At present, relevant research on intestinal flora of gynogenetic progeny derived from hybridization between carnivorous and omnivorous fish is still insufficient.

The fish intestine is the core organ responsible for nutrient digestion and absorption, and intestinal microbiota is closely linked to host growth performance and energy metabolism. The diversity of intestinal microorganisms increases gradually with fish development, even the structure and abundance of intestinal microflora vary in fish at different growth stages [12] and growth rates [13]. The abundance of Actinobacteria in largemouth bass with fast growth rates is higher than that in largemouth bass with slow growth rates [14]. The growth of the host can be measured by the ratio of *Firmicutes/Bacteroides* [15]. Intestinal flora mainly regulates the interaction between host organs and tissues by metabolizing short-chain fatty acids (SCFA) [16, 17] to improve the weight gain rate. SCFA can also be used to promote host mitochondrial fatty acid oxidation and energy consumption [18], and regulate signaling pathways by activating free fatty acid receptors to consume energy [19]. However, there is no universal correlation model between intestinal flora and host growth or energy metabolism across fish species. For hybrid fish (including distant hybrids and gynogenetic progeny), the causal relationship and molecular mechanism between intestinal flora and host energy metabolism have not been fully elucidated.

Gynogenesis is a powerful breeding technique. Previous studies have shown that a small amount of paternal genetic material will be integrated into the gynogenesis to produce progeny during the process of heterologous sperm induction, and this phenomenon is called “micro-hybrid”. These paternal fragments may contribute to genetic variation and it is also highly likely that the progeny will acquire certain favorable traits [20, 21]. Gynogenesis can induce microhybridization in offspring and produce dominant traits. This phenomenon has been confirmed in various fish species [22] such as disease-resistant grass carp [20] and gynogenic blunt snout bream (GBSB). Offspring with partial paternal traits can be obtained via physical or chemical treatments (e.g., cold shock and colchicine treatment) [23]. They may exhibit stronger disease resistance [24, 25], faster growth rates [26], or greater tolerance to hypoxia [27] than their maternal parents. In addition to micro hybridization, distant hybridization is employed to hybridize fish with different feeding habits [21, 28] and obtain offspring with enhanced economic benefits and aquaculture prospects [29, 30]. Offspring obtained through distant hybridization between herbivorous (or omnivorous) female blunt snout bream × carnivorous male topmouth culter (*Culter alburnus*, TC) have been extensively studied [31]. Although the diet of natural gynogenic blunt snout bream (GBSB) is mainly influenced by the maternal parent, the paternal parent also affects sequence variation and gene expression in the offspring [32]. Meanwhile, the genetic (subgenomic) information of the host significantly changes the intestinal characteristics (structure, relative intestinal length [33], relative intestinal mass, and Zihler index) and intestinal microbiota composition [34] of the heterozygous offspring. In our previous studies, we found that the hybrid offspring of omnivorous BSB and carnivorous mandarin fish have faster growth rates than the maternal

offspring and that their growth is significantly related to the upregulated expression of growth-related factors (e.g., myogenic regulatory factors) in muscle [35]. However, the gut characteristics and gut microbiota of natural gynogenetic offspring from omnivorous and carnivorous parents have not been characterized.

We speculate that the intestinal morphology, digestive/antioxidant enzyme activity, intestinal microbial composition and glucose metabolism gene expression may change in the offspring obtained by crossing between carnivorous fish and omnivorous fish, which may enhance digestion performance compared with maternal. To determine the effect of hybridizing fish with different feeding habits on the intestinal flora of gynogenic offspring [2], we measured the intestinal structures of GBSB, BSB, and Chinese perch (CP) and compared their intestinal microbial diversity. In addition, we assessed the expression of intestinal growth and metabolic genes, mainly includes *Pgd*, *Idha*, *sdha*, and 12 other related genes through quantitative PCR analysis, and analyzed their correlation with intestinal flora. The results of this study provide insights into the functional mechanism of the intestinal microflora of gynogenic fish hybridized from carnivorous and omnivorous parents. This study may serve as a basis for improving the yield and quality of aquaculture.

Materials and methods

Ethics statement

This research complied with the Guide for the Care and Use of Laboratory Animals of Hunan Normal University. Fish samples were anesthetized with 100 mg/L MS-222 (Sigma) before dissection.

Gynogenesis and sampling

The experiment was conducted at the Fish Breeding Base in Wugang, Hunan, China. Twenty each of sexually mature BSB and CP were randomly selected as parents between May and July 2023. Sperm and eggs were mixed for fertilization, and the fertilized eggs were incubated in water at 22–25 °C, which produced GBSB fry. The hatched GBSB fry were reared at a density of 400 per acre in a pond with Ph 7.0–7.2 and dissolved oxygen of about 6.5 mg/L. The fish were fed a commercial feed twice a day, about 5% of the total weight of the fish. The specific production process and feeding situation of GBSB can be referred to [36]. In the experimental group with *Megalobrama amblycephala* as the female parent and *Siniperca chuatsi* as the male parent, the fertilization rate was 23.18%, the hatching rate was 2.83%, and the malformation rate was 77.96%. Refer to our team 's previous verification results, the higher malformation rate of gynogenetic offspring is due to the incomplete replication or abnormal development of the genome caused by the natural gynogenesis of heterologous sperm [37]. Only normal and healthy individuals were used for subsequent analysis. However, no surviving offspring were obtained from the distant hybridization experiment using male *M. amblycephala* and female *S. chuatsi*. Meanwhile, the sexually mature BSB and CP were self-crossed to produce normal BSB and CP offspring, respectively. The gynogenetic nature of GBSB was confirmed by flow cytometry (diploidy, 2n = 48) and microsatellite analysis, which detected maternal-specific alleles and the presence of a few paternal-specific fragments, consistent with microhybridization [37, 38]. We referred to previous studies and used the same group of verified fish.

Three types of fish were placed in three ponds (2 ha and depth 3 m) with suitable density, pH (7.0–8.5), water temperature (22–24 ◦C), dissolved oxygen content (5.0–8.0 mg/L) and adequate forage. And with each pond divided into six grid cages. The CP is fed with sufficient bait fish, and the length of the bait fish is one-third of the length of the CP. BSB and GBSB are fed with commercial feed. Thirty age-matched fish with no significant difference in body weight were randomly selected from the six grid cages of the three fish species. We selected 12-month-old fish, both sexes were included. The samples were collected after 24 h of fasting. Six fish were randomly selected in each group (BSB, GBSB, and CP). The fish surface was wiped with a 70% alcohol-soaked cotton ball, and dissection was performed with sterile dissection tools around the alcohol lamp. A portion of the

removed intestinal sample was soaked in 4% paraformaldehyde for histological analysis; another portion of the intestinal sample was washed with cold sterile 1 × PBS to remove contaminating blood. For autophagy anatomy analysis, the gut samples were fixed in 5% glutaraldehyde buffer, embedded for more than 24 h, and then used for the analysis of mitochondrial damage. Another portion of intestinal tissue was snap-frozen and then stored in a –80 °C ultra-low temperature freezer until analyses of gene expression, protein content, and enzyme activity. For intestinal microbiota analysis, metagenomic sequencing was performed, and the intestinal contents were removed and transferred to 2 mL sterile centrifuge tubes, frozen with liquid nitrogen, and then stored in a –80 °C ultra-low temperature freezer until DNA extraction.

Histological examination of the intestine

Fixed samples of BSB, GBSB, and CP (six replicates each) were subjected to sequential processing, which included alcohol washing and dehydration, clearing, paraffin embedding, sectioning, mounting, dewaxing, hematoxylin–eosin staining, dehydration, clearing, and sealing. All samples were taken from the mid-intestine for analysis. The same region was used for each individual to ensure consistency. Microscopic observation and imaging were performed to examine intestinal morphological structures. Key histological parameters, including villus height, villus width, villus density, and intestinal wall thickness, were measured and compared between GBSB and its parental strains to analyze differences in intestinal morphology [39].

Mitochondrial damage analysis of intestinal samples

Transmission electron microscopy (TEM) images of the immobilized gut samples of GBSB, BSB, and CP were obtained using a transmission electron microscope. The number of autolysosomes was counted artificially at a certain magnification, and their cytoplasmic areas were quantified using ImageJ software.

Multiple assays for intestinal digestive and antioxidant-related molecules

To determine the activities of various enzymes in the intestine, approximately 1 g of sample (six replicates per species) was homogenized on ice with 10 volumes (w/v) of ice-cold physiological saline and then centrifuged at 4 °C and 1800 g for 15–20 min. The resulting supernatant was stored at −80 °C and used for multiple enzyme activity assays with kits provided by the Nanjing Jiancheng Bioengineering Institute. Total protein content was analyzed using the bicinchoninic acid method. The activities of digestion-related enzymes, including α-amylase (AMS), acid phosphatase (ACP), lipase (LPS), cellulase (CL), alkaline xylanase (BAX), and acid xylanase (ACX) were assessed. AMS activity was determined by measuring the blue complex formed from the starch–iodine reaction at 660 nm using a spectrophotometer. ACP activity was measured indirectly at 520 nm based on the formation of a red quinone derivative from free phenol (produced in the ACP-catalyzed reaction) reacting with 4-aminoantipyrine under alkaline conditions and oxidized by potassium ferricyanide. LPS activity was evaluated by monitoring the rate of decrease in scattered light or turbidity due to the hydrolysis of triglyceride-containing micelles. CL activity was calculated from the maximum absorbance at 550 nm of the brown–red amino compound generated when reducing sugars produced in the reaction reduced 3,5-dinitrosalicylic acid (DNS) under alkaline conditions. BAX and ACX activities were determined from the rate of increase in absorbance at 540 nm due to the color reaction between reducing oligosaccharides and monosaccharides (released from xylan degradation under alkaline or acidic conditions, respectively) and DNS in a boiling water bath. The levels of antioxidants, including malondialdehyde (MDA), superoxide dismutase (SOD), zinc–copper superoxide dismutase (CuZn-SOD), catalase (CAT), and reduced glutathione (GSH) were also measured. MDA content was calculated from the maximum absorbance at 532 nm of the red product formed by its condensation with thiobarbituric acid (TBA). SOD and CuZn-SOD activities were measured by the change in absorbance caused by nitrite reduction, which occurs due to the specific inhibition of superoxide anion radicals when SOD is present. CAT activity was calculated from the change in

absorbance at 405 nm resulting from the light-yellow complex formed between residual hydrogen peroxide and ammonium molybdate. GSH content was quantified colorimetrically at 405 nm by measuring the yellow product generated from its reaction with 5,5'-dithiobis- (2-nitrobenzoic acid).

Bioinformatics metagenomic analysis of the intestine

Microbial DNA was extracted from the intestinal contents of six individual samples each of GBSB, BSB, and CP using an improved CTAB method. DNA quality was assessed by 1% agarose gel electrophoresis and pulsed-field gel electrophoresis, and quantification was performed using a Nanodrop kit and a Qubit® 2.0 Fluorometer. The samples were shipped on dry ice to Novogene Co., Ltd. (Beijing) for sequencing. Sequencing data has been deposited in the NCBI Sequence Read Archive (SRA) database(https://dataview.ncbi.nlm.nih.gov/object/PRJNA1303868?reviewer=a4jgu04vrhtndhd55vjp41haqs) under BioProject ID PRJNA1303868 accession numbers SAMN50539832 to SAMN50539840. Illumina PE150 was used for sequencing. After sequencing, the raw data was subjected to quality control and host filtering to remove reads containing low-quality bases (mass value< =38) exceeding a certain proportion (default set to 40bp). Bowtie2 (v2.2.4) software (parameter settings: -end-to-end, -sensitive, -I 200, -X 400) was used to filter host-contaminated reads. Use MEGAHIT (v1.0.4) assembly software for assembly analysis (assembly parameter: -presets meta-large) to filter out fragments below 500 bp. MetaGeneMark (v2.10) was used to predict ORF (Open Reading Frame), and the information with a length of less than 100 nt was filtered out. CD-HIT (v4.5.8) software was used to remove redundancy. By default, 95% identity and 90% coverage were used for clustering. The species annotation information of each gene was obtained by comparing with the MicroNR library. Functional annotation and abundance analysis of metabolic pathway (KEGG), homologous gene cluster (eggNOG), carbohydrate enzyme (CAZy) were performed.

qPCR analysis of intestinal glucose metabolic genes in BSB, GBSB, and CP

In each experimental group, six intestinal tissue samples were collected for analysis. RNA was extracted from the gut specimens using Trizol reagent (Sangon), after which first-strand cDNA synthesis was carried out using the PrimeScript RT Kit (Monad). The investigation focused on genes associated with growth and metabolism, particularly *Pgd*, *Idha*, *sdha,* and 12 other related genes through quantitative PCR analysis. Six candidate reference genes (β-actin, GAPDH, 18S rRNA, EF1a, RPL13a, rps29) were evaluated using the online tool RefFinder (http://blooge.cn/RefFinder/, accessed on January 23, 2026). β-actin was selected as the most stable and used for normalization. BSB and GBSB use the same set of primers, and CP uses another set of primers. Primer sequences for the selected reference gene and all target genes are provided in Table S1. Gene-specific primers were designed using Primer Premier 5 software to amplify the target mRNA sequences (Table S1), with all primers commercially synthesized by Sangon Biotech Co., Ltd. The qPCR protocol involved an initial predenaturation step at 95 °C for 30 s, followed by 40 cycles of denaturation at 95 °C for 10 s and annealing at 60 °C for 30 s. Melt curve analysis was performed to verify amplification specificity. The amplification efficiency (E) of the other 15 candidate genes related to glucose metabolism ranged from 90 to 110%. For each of the six biological replicates per group, two independent qPCR reactions were performed. Each of these duplicate reactions was run with three technical replicates. The mean Ct value of the three technical replicates was used as the value for each biological replicate. Quantitative analysis of gene expression levels was conducted using the $2^{-\Delta\Delta Ct}$ method [40].

Correlation analysis of intestinal microbes and expression of glucose metabolic genes

Pearson correlation analysis was employed to assess the relationships between the functional abundance of gut microbiota and the expression levels of intestinal glucose metabolism-related genes. The microbial abundance data were normalized by Reads Per Million (RPM), and genus-level relative abundances were then log10-transformed. To account for multiple testing, the Benjamini–Hochberg false discovery rate (FDR) correction was

applied, and correlations with an adjusted Q-value were considered statistically significant. "*" indicates that $q<0.05$ reaches a significant level; "**" indicated that $q<0.01$ reached a very significant level. The correlation coefficient r reflects the direction and intensity. Red is positive and blue is negative. The deeper the color, the greater the intensity. Bioinformatic analyses were performed using R version 4.5.1 (including packages such as ggplot2 and pheatmap) to analyze the data and generate clustered heatmaps.

Statistical analysis

Prior to one-way ANOVA, normality was assessed using the Shapiro–Wilk test, and homogeneity of variances was verified by Levene's test. Data that did not meet normality assumptions were log10-transformed. Statistical analyses were performed using SPSS 20.0. All data are presented as the mean ± SEM (n = 6). Differences were analyzed by one-way ANOVA followed by Duncan's multiple range test. Statistical significance was considered at $*p<0.05$ and $**p<0.01$.

Results

Histological analysis of the intestine in BSB, GBSB, and CP

The intestinal characteristics of GBSB and its parents (BSB and CP) were compared to assess the impact of genetic diversity and genomic interactions on intestinal structure and morphology (Fig. 1). Microscopic examination results indicated that the maternal parent (BSB) exhibited the highest number of intestinal villi, which were longer and straighter. This elongated and narrow intestinal morphology is typically associated with efficient nutrient absorption. Among the three species, CP exhibited the greatest muscular thickness and intestinal villus width, which enabled it to rapidly propel food through the intestine and provided an advantage in the ingestion and digestion of high-energy foods. The villus density of GBSB may be influenced by the paternal heterosis

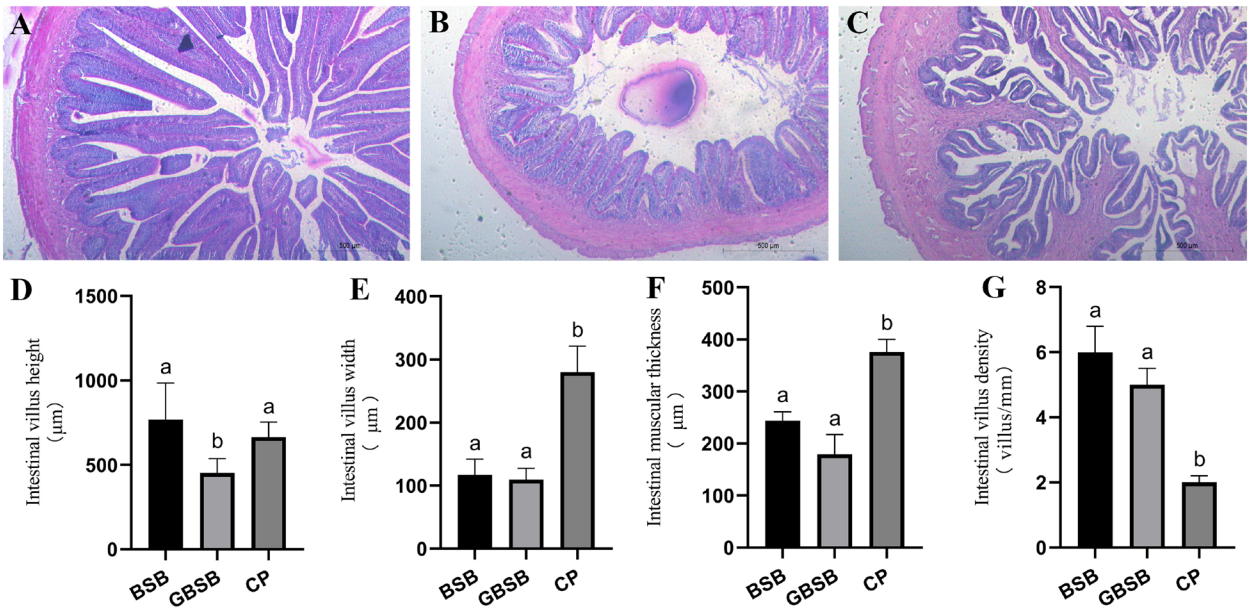


Fig. 1 Photomicrographs of intestinal sections in BSB, GBSB, and CP, respectively. **A** BSB; **B** GBSB; **C** CP. Comparison of intestinal morphological indicators among the three types of fish, respectively. **D** intestinal villus height; **E** intestinal villus width; **F** intestinal muscular thickness; **H** intestinal villus density. Data are presented as mean ± standard deviation of the mean (n = 6). Statistical differences among the three groups are indicated by different letters in lowercase ($p<0.05$)

effect, whereas the narrower villus width and smallest muscular thickness aligned more closely with the maternal genetic traits.

Mitophagy status of the intestine in BSB, GBSB, and CP

The intestinal oxidative damage in GBSB, BSB, and CP was visualized via TEM to reveal their ultrastructural characteristics (Fig. 2). Quantitative analysis showed that the average number of autophagosomes per unit area in the GBSB and BSB groups was 3.3 ± 0.57. This number was significantly higher ($p < 0.05$) than that in the paternal CP group, which had only 2 autophagosomes per unit area.

Comparative analysis of gut digestive enzyme activities in BSB, GBSB, and CP

To investigate the changes in intestinal digestive enzyme activities of gynogenic offspring derived from parents with different feeding habits, we detected several gut digestive enzyme-related molecules in BSB, GBSB, and CP (Fig. 3). Compared with the BSB group, the GBSB group showed significantly higher activities of BAX, ACP, and LPS and significantly lower CL and AMS activities. Compared with the CP group, the GBSB group exhibited higher CL and AMS activities. Results from digestive enzyme activity assays demonstrated that gynogenically produced omnivorous GBSB displayed enhanced activities of BAX, ACP, and LPS.

Analysis of gut antioxidant-related molecules in BSB, GBSB, and CP

To explore the changes in the intestinal antioxidant capacity of the gynogenic offspring of parents with different feeding habits, we detected some antioxidant-related molecules in the intestines of BSB, GBSB, and CP (Fig. 4). The contents of MDA were lower in GBSB than in CP and BSB. The intestinal activities of CAT, CuZn-SOD, and GSH in GBSB were higher than those in BSB but lower than those in CP. However, the SOD activity in GBSB was significantly lower than that in BSB.

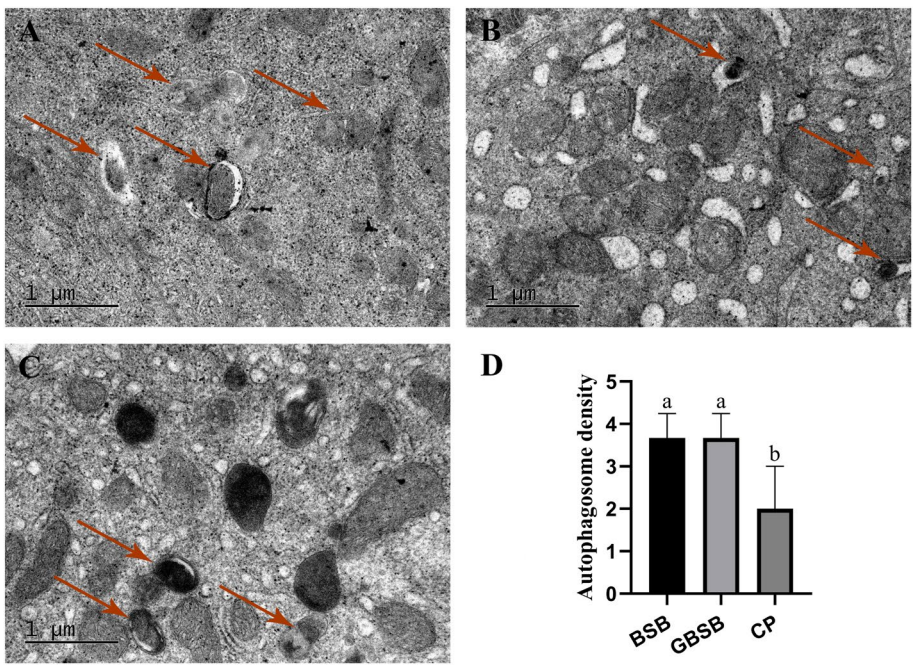


Fig. 2 Ultrastructural analysis of intestinal tissues by TEM: **A** BSB, **B** GBSB, **C** CP. Red arrows indicate autophagosomes; **D** Statistical analysis of autophagosome density among the three fish groups. Data are presented as mean ± standard deviation of the mean (n = 6). Statistical differences among the three groups are indicated by different letters in lowercase ($p < 0.05$)

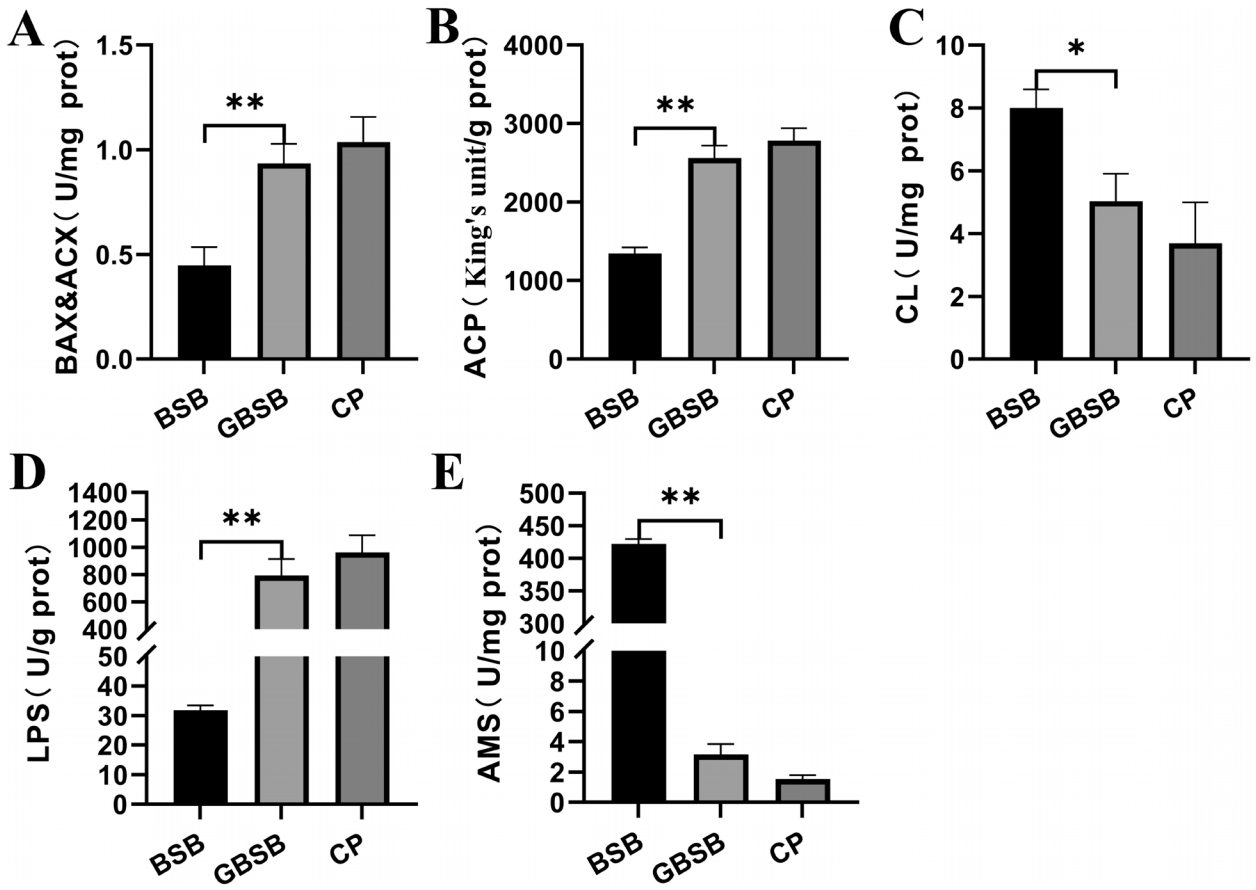


Fig. 3 Gut digestive enzyme activities in BSB, GBSB, and CP. The bar graphs show the activity of soil basic xylanase (BAX) in BSB and GBSB and acidic xylanase (ACX) in CP (**A**), acid phosphatase (ACP) (**B**), cellulase (CL) (**C**), lipase (LPS) (**D**), and amylase (AMS) (**E**). Data are presented as mean ± standard deviation of the mean (n = 6). Statistical differences among the three groups are indicated by different letter notations ($p < 0.05$). *$p < 0.05$, **$p < 0.01$

Operational taxonomic unit composition and structure at the phylum and genus levels of the gut microbiota in BSB, GBSB, and CP

To compare the gut microbiota composition and diversity of GBSB and its parental strains, we performed a sequencing analysis of their unique and shared operational taxonomic units (OTUs) (Fig. 5A). The total number of OTUs unique to or shared among the three fish species was 899,873. Specifically, BSB, GBSB, and CP possessed 678,768, 519,576, and 138,683 OTUs, respectively, with 32,305 OTUs shared by all three. The number of OTUs shared uniquely between GBSB and BSB was 328,774, which was significantly higher than the 7,726 OTUs shared uniquely between GBSB and CP (Fig. 5A).

The metagenomic sequencing data were used to create functional abundance clustering heatmaps at the phylum and genus levels for the gut microbiota in BSB, GBSB, and CP to reveal the functional/structural differences of the gut microbiota under different diets. The CP group exhibited dominant microbiota primarily consisting of *Clostridium*, *Plesiomonas*, *Edwardsiella*, and *Cetobacterium*. The BSB group displayed a microbial composition characterized by *Pseudoalteromonas*, *Bacillus*, *Turicibacter*, and *Culicoidibacter*. Notably, the offspring GBSB group demonstrated maternal inheritance traits (evidenced by the high abundance of *Bacillus*) and the emergence of novel dominant genera, including *Vibrio*, *Aeromonas*, and *Romboutsia*. This result indicated that the offspring's microbial community was shaped by the combined effects of parental genetic and environmental factors (Fig. 5B).

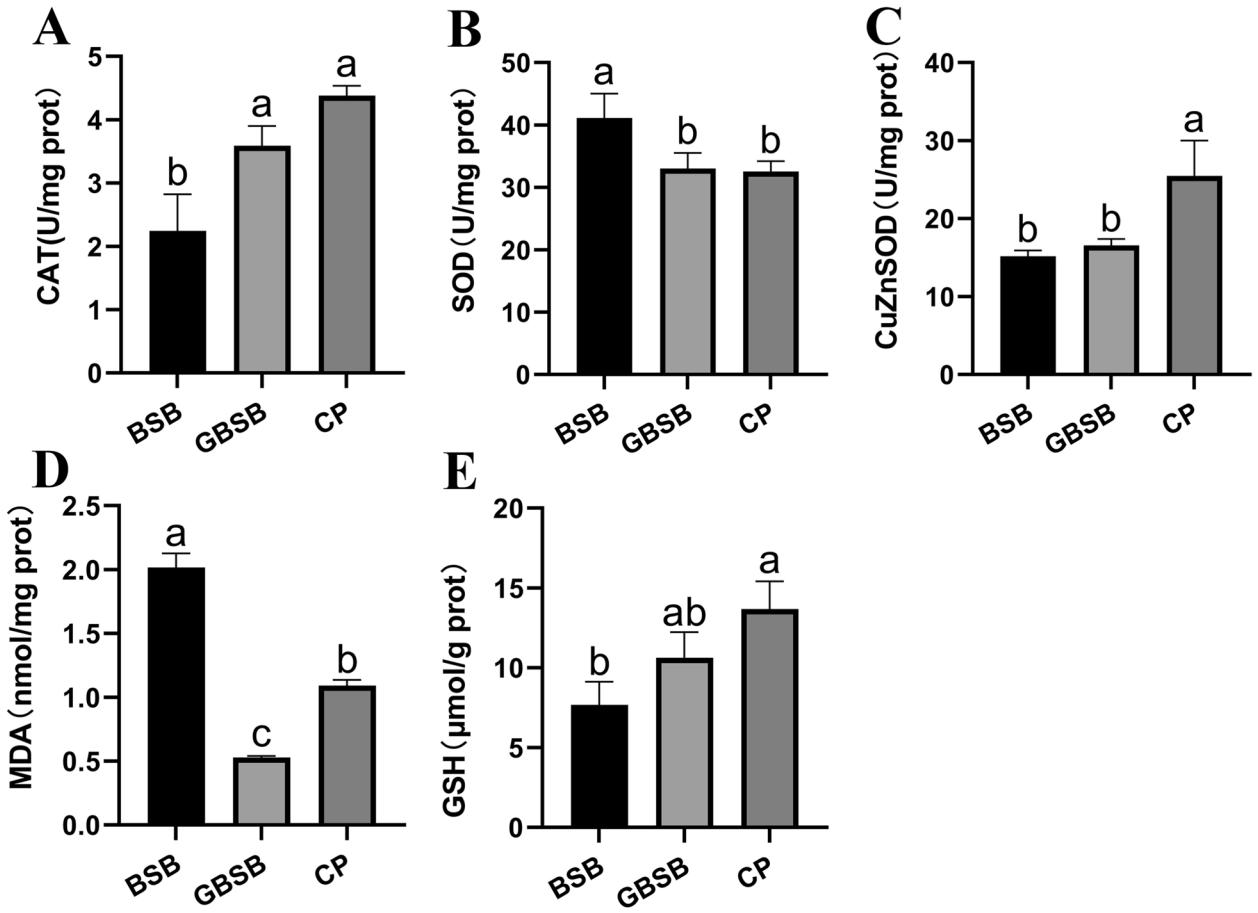


Fig. 4 Gut antioxidant-related molecules activities of BSB, GBSB, and CP. The bar graphs show the activities of malondialdehyde (MDA) (**A**), catalase (CAT) (**B**), superoxide dismutase (SOD) (**C**), copper-zinc superoxide dismutase (CuZn-SOD) (**D**), and glutathione (GSH) (**E**). Data are presented as mean ± standard deviation of the mean (n = 6). Statistical differences among the three groups are indicated by different letters in lowercase ($p < 0.05$)

Expression of intestinal glucose metabolic genes in BSB, GBSB, and CP

To analyze the expression levels of intestinal glucose metabolic genes in GBSB and its parental species, we measured the mRNA levels of 15 genes, including *GAPDH*. The expression of glycolysis-related genes in CP was significantly lower than that in the omnivorous BSB and GBSB. Notably, the expression levels of *GAPDH* and *Idha* in GBSB were significantly lower than those in BSB, showing intermediate levels between the two parental species (Fig. 6A). However, in the pentose phosphate pathway (PPP) and glycogen metabolism, the expression of *Prkaa* in the CP group was significantly higher than that in the other two groups, with GBSB exhibiting significantly higher *Pgd* expression than BSB (Fig. 6B). In the tricarboxylic acid cycle pathway, the expression levels of *Cs*, *Ogdh*, and *sdha* in the CP group were significantly higher than those in the other two groups, whereas the expression of *sdha* in GBSB was significantly higher than that in its maternal parent. Conversely, the expression levels of *Aco2*, *suclg1*, and *sdhc* in BSB were significantly higher than those in the other two groups, with GBSB showing significantly higher expression of *suclg1* and *sdhc* than its paternal parent. Furthermore, the expression of *Mdh2* in GBSB and its maternal parent was significantly higher than that in CP (Fig. 6C).

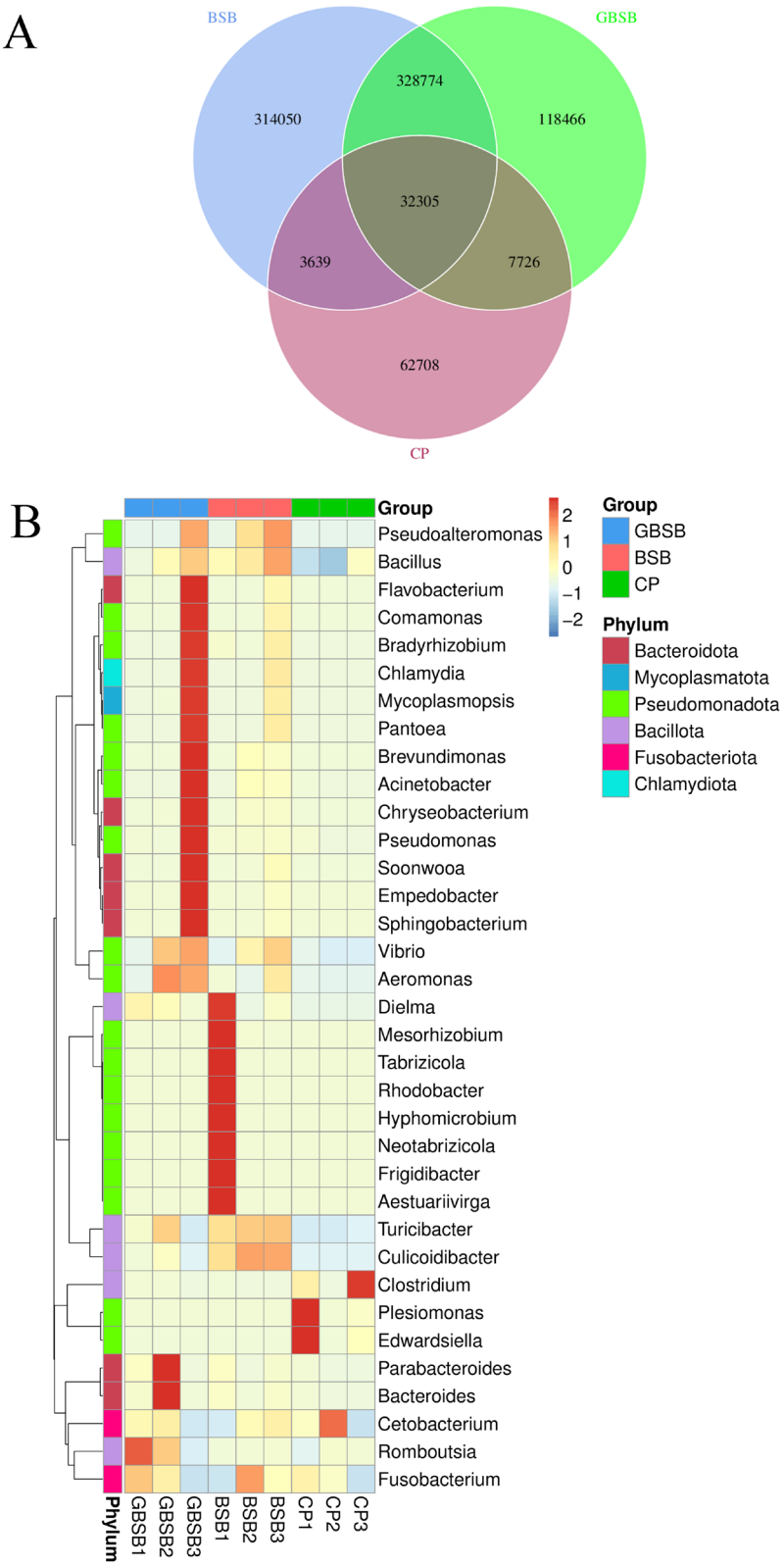


Fig. 5 **A** Venn diagram of OTU distribution in BSB, GBSB, and CP; **B** Clustering heatmap of functional abundance of intestinal bacterial communities in GBSB, BSB, and CP at the phylum and genus levels

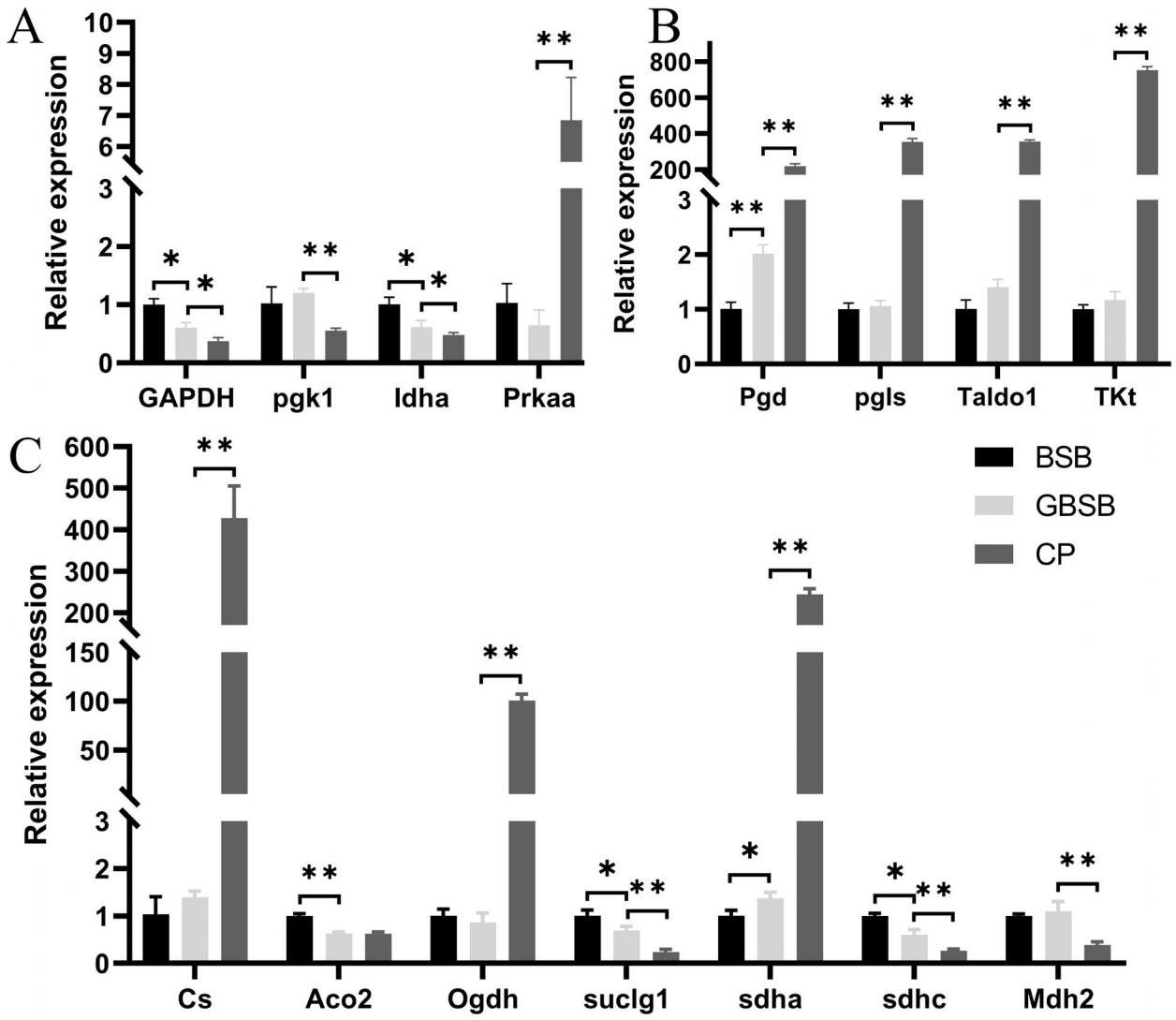


Fig. 6 A Differential expression of glycolysis and glycogen metabolic genes in BSB, GBSB, and CP; **B** Differential expression of pentose phosphate pathway (PPP) genes in BSB, GBSB, and CP; **C** Differential expression of tricarboxylic acid cycle (TCA) genes in BSB, GBSB, and CP. Values are expressed as the mean ± standard deviation (n = 6) of the normalized transcript levels of each gene. Statistical differences between time points are indicated by different letter notations ($p < 0.05$). *$p < 0.05$, **$p < 0.01$. The numbers on the graph represent the amplification of the relative expression of the gene directly below

Correlation analysis of intestinal microbes and glucose metabolic gene expression in BSB, GBSB, and CP

Pearson correlation analysis and correlation clustering heatmaps revealed that in BSB intestines, the expression levels of glycolytic genes *GAPDH* and *ldha* were significantly positively correlated with the functional abundance of *Brevundimonas* but significantly negatively correlated with that of *Edwardsiella*; *pgk1* was significantly positively correlated with *Edwardsiella* and significantly negatively correlated with *Acinetobacter*; *Cs* was significantly positively correlated with *Dielma* and significantly negatively correlated with *Culicoidibacter*; *Aco2* was significantly positively correlated with *Bacteroides*; *Oghd*, *Taldo1*, and *Tkt* were all significantly negatively correlated with *Pseudoalteromonas*, with *Ogdh* showing an extremely significantly negative correlation with *Vibrio*; *suclg1* and *sdha* were significantly negatively correlated with *Turicibacter*; Prkaa was significantly positively correlated with *Clostridium*; *Pgd* was significantly negatively correlated with *Romboutsia*; *pgls* was significantly

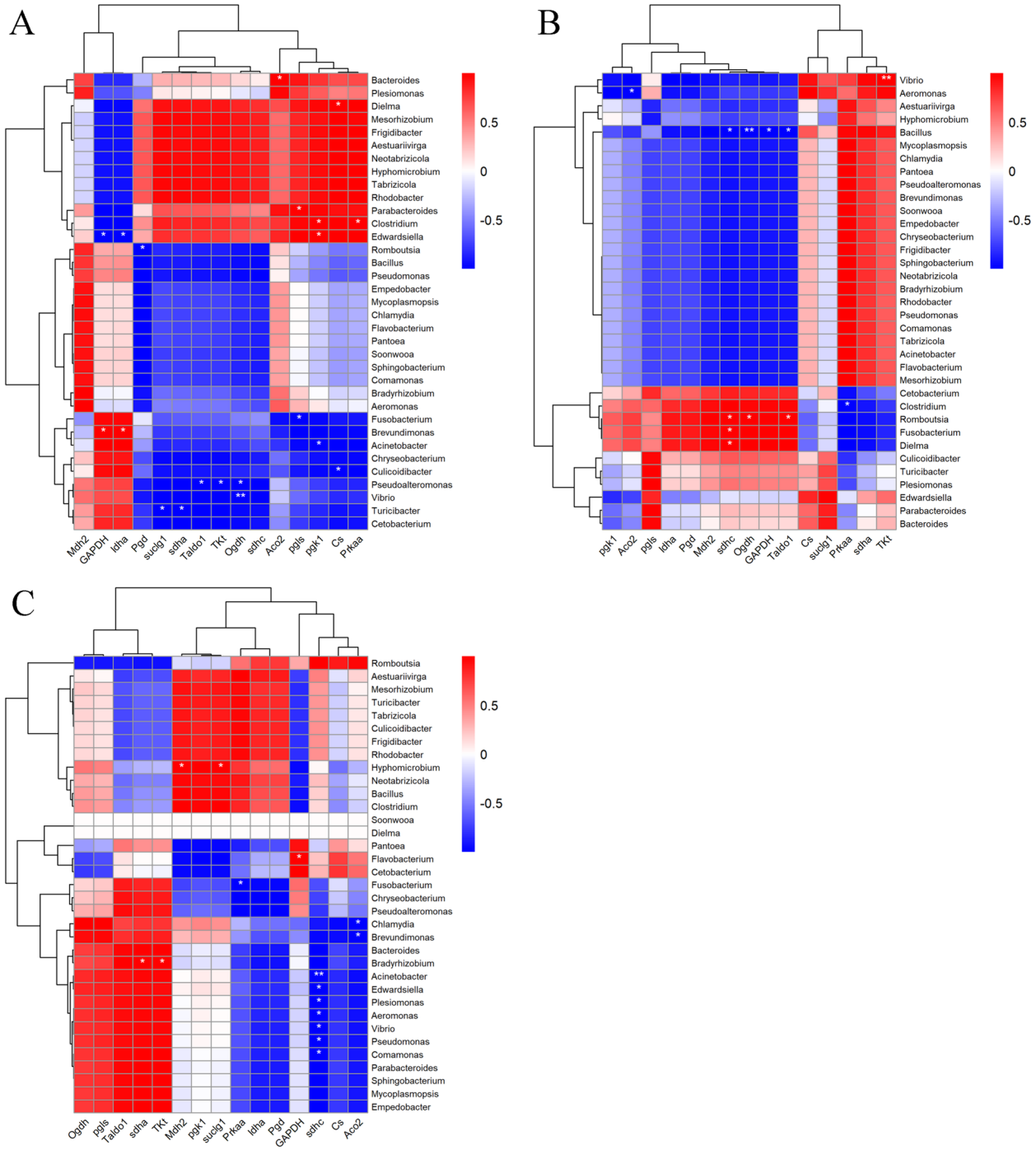


Fig. 7 Correlation heatmaps between intestinal bacterial genera and glucose metabolism-related gene expression in **A** BSB, **B** GBSB, and **C** CP. The correlation coefficient r reflects the direction and intensity. Red is positive and blue is negative. The deeper the color, the greater the intensity. Genus abundances were log10-transformed prior to analysis. Only correlations with Benjamini–Hochberg FDR-adjusted Q-values are shown. *q < 0.05, **q < 0.01

positively correlated with *Parabacteroides* and significantly negatively correlated with *Fusobacterium* (Fig. 7A). In GBSB intestines, the expression level of the glycolytic gene *GAPDH* was significantly and negatively correlated with the functional abundance of *Bacillus*. *Aco2* expression was significantly negatively correlated with *Aeromonas*. Meanwhile, *Oghd*, *sdhc*, and *Taldo1* were all significantly positively correlated with *Romboutsia*

but significantly negatively correlated with *Bacillus*. Notably, *Oghd* strongly negatively correlated with *Bacillus*. Additionally, *sdhc* was significantly positively correlated with *Fusobacterium* and *Dielma*, whereas *Prkaa* was significantly negatively correlated with *Clostridium*. *Tkt* was very strongly positively correlated with *Vibrio* (Fig. 7B). In CP intestines, the expression level of the glycolytic gene *GAPDH* was significantly and positively correlated with the functional abundance of *Flavobacterium*; *Aco2* was significantly negatively correlated with *Chlamydia* and *Brevundimonas*. Furthermore, *suclg1* and *Mdh2* were significantly positively correlated with *Hyphomicrobium*, whereas *sdha* and *Tkt* were significantly positively correlated with *Bradyrhizobium*; *sdhc* was significantly negatively correlated with *Comamonas*, *Plesiomonas*, *Vibrio*, *Aeromonas*, *Pseudomonas*, and *Edwardsiella* but very strongly negatively correlated with *Acinetobacter*; *Prkaa* was significantly negatively correlated with *Fusobacterium* (Fig. 7C).

Discussion

To investigate the gut microbiota of gynogenic offspring GBSB derived from the omnivorous maternal BSB and the carnivorous paternal CP, we analyzed their intestinal histomorphology, gut microbiota, and digestive and antioxidant-related enzyme activities. We also quantified the expression of glycolysis-related genes in the intestines of GBSB and its parents, and performed Pearson correlation analysis between the functional abundance of gut microbiota and the expression levels of glycolysis-related genes. The results showed that intestinal morphology differed among groups, consistent with feeding habits. At the molecular level, enzyme activities and transcriptional profiles of glucose metabolism-related genes revealed differences between GBSB and its parents. Correlation analyses further suggested associations between gut microbiota composition and host gene expression, providing correlational evidence for potential microbiota–host interactions in intestinal metabolic regulation.

This study measured intestinal villus height, width, density, and muscle thickness in GBSB and its parents. The carnivorous CP had significantly higher intestinal muscle thickness and villus width than the omnivorous BSB and GBSB. The villus density of GBSB was intermediate between the parents but closer to the omnivorous parent BSB, whereas its villus width and muscle thickness showed no significant difference from the omnivorous maternal parent, consistent with previous conclusions. Additionally, TEM results revealed that the average number of autophagosomes per unit area in the GBSB group did not differ significantly from that in the BSB group but was significantly higher than that in the CP group. This result suggests that intestinal autophagy regulation is also primarily influenced by the omnivorous maternal parent [41, 42]. Meanwhile, the intestinal activities of CAT and GSH in GBSB were significantly higher than those in BSB. MDA content was significantly lower in GBSB than in BSB. This result is consistent with the relevant findings on GBSB muscle, showing that the antioxidant enzyme activity in GBSB muscle and gut is higher than that in BSB. This finding may also be due to the insertion of heterologous gene fragments, resulting in differences in intestinal antioxidant enzyme activity between GBSB and BSB [38]. This study found that the ACP and LPS activities of the carnivorous parent CP were the highest, whereas CL and AMS showed the lowest compared with BSB and GBSB. This model is consistent with the typical characteristics of carnivorous fish with high LPS and low AMS, which is consistent with its high protein and high fat diet, and further supports the conclusion that digestive enzyme activity is closely related to diet [43]. Notably, the four digestive enzyme activities of GBSB were significantly different from its omnivorous female parent, but more similar to the carnivorous male parent. It is speculated that the LPS activity of the gynogenetic offspring is affected by the micro-hybrid effect, so that the fat digestion and absorption efficiency is significantly higher than that of the maternal parent. Combined with metagenomic sequencing results, we speculated that GBSB not only has a stable source of xylanase influenced by the maternal parent but also utilizes relevant functions of ingested bacterial strains affected by the paternal parent, explaining the significantly higher intestinal BAX activity in GBSB than in BSB.

Previous studies have found that carnivorous fish generally rely on protein metabolism, whereas omnivorous fish exhibit a higher capacity for glucose metabolism than carnivorous species [44]. In the present study, the

expression level of glycolysis-related genes in the carnivorous parent CP was the lowest among the three groups; the expression of glycolysis genes (*GADPH*, *Idha*) and TCA cycle genes (*Aco2*, *suclg1*, *sdha/c*) in the gynogenetic offspring GBSB were between the parents, and the expression of *sdha* was higher than that of the female parent. It is speculated that this phenomenon is due to the regulation of carnivorous paternal parents, which up-regulates the expression of *sdha* to regulate the response of TCA cycle to different substrate sources, thereby enhancing the adaptability to broad-spectrum diet [45, 46]. Furthermore, the expression levels of PPP-related genes in GBSB were higher than those in the maternal parent, with the key enzyme gene *Pgd* being significantly higher. In summary, GBSB may be influenced by the allopaternal genetic effects of certain gene fragments from the paternal parent, leading to the downregulated expression of some glucose metabolism-related genes and a consequent reduction in glycolytic capacity.

Consistently, both omnivorous BSB and GBSB had higher operational taxonomic unit (OTU) richness based on sequence similarity than carnivorous CP [47]. Furthermore, the number of OTUs shared between GBSB and BSB was greater than that between GBSB and CP, indicating that GBSB is more similar to BSB not only in feeding habits but also in gut microbial environment. This seems to have a similar effect to the maternal inheritance of gynogenesis [37]. The dominant bacteria in the intestine of the three fish species were Pseudomonadota and Bacillota, but the functional abundance was different. Although the abundance of Fusobacteriota in the GBSB intestine is low, it is positively correlated with most sugar metabolism genes and may be affected by the paternal parent. Functional abundance heatmaps revealed that GBSB and BSB harbored *Bacillus*, a common dominant genus in omnivorous fish. Furthermore, correlation analysis showed that the functional abundance of the Firmicutes genus *Bacillus* in the BSB intestine was positively correlated with the glycolysis-related gene *GAPDH* and the lactate metabolism-related gene *Idha*. The abundance of Bacteroidota was highest in GBSB among the three fish species, even exceeding that of the maternal group. In the present study, *Parabacteroides*, *Bacteroides*, and *Aestuariivirga*, all of which belong to Bacteroidota in the BSB intestine, were positively correlated with almost all sugar metabolism-related genes, but in GBSB were retained partial positive correlations. The abundance of *Vibrio* in GBSB was higher and negatively correlated with glycolytic genes, which may be due to nutritional competition. *Romboutsia* positively correlated with the expression of most glucose metabolism-related genes in the GBSB intestine. However, no existing research on *Romboutsia* and glucose metabolism aligns with the current findings, and the underlying mechanism requires further investigation. Overall, we speculate that the growth rate and meat content of the gynogenic offspring are higher than those of the maternal parent because the gut microbiota affects the metabolic mode of GBSB, resulting in stronger nutrient absorption of the gynogenic offspring than the maternal parent [35]. Meanwhile, this gut microbiota–host glucose metabolism interaction may contribute to enhances microbial richness in gynogenic offspring while potentially altering microbial regulatory mechanisms and increasing the risk of intestinal dysbiosis. However, these changes were only observed at the transcriptional level; In order to confirm functional metabolic reprogramming, metabolite flux needs to be directly measured. Overall, glucose metabolism is a complex physiological process involving multiple factors, and the specific mechanisms underlying these relationships require further exploration and validation. There are still some limitations in this study. In order to make the data more reliable, we need to study a larger sample size in the future. Secondly, the relationship between gut microbiota and host gene expression we observed may be affected by unmeasured confounding factors. Thirdly, there is no metabolomics analysis in this manuscript, and the functional mechanism linking the microbiota to glucose metabolism is still speculative. Therefore, our future research should integrate metabolomics and genomics models for more rigorous analysis.

Conclusion

In this study, the natural gynogenic blunt snout bream (GBSB) demonstrates superior intestinal characteristics compared with the common blunt snout bream (BSB). The main findings of this study are as follows: a) GBSB exhibits higher intestinal antioxidant enzyme activities and digestive enzyme activities than BSB, indicating

enhanced intestinal antioxidant capacity and digestive ability; b) The expression levels of PPP metabolism-related genes in the intestines of gynogenic offspring are intermediate between those of the parents and higher than those of the maternal parent; c) The richness of the intestinal microbiota in GBSB is greater than that in BSB; d) The correlations between the intestinal microbiota of GBSB and genes involved in multiple pathways of glucose metabolism are more diverse than those in the parental BSB. Through the distant hybridization of omnivorous BSB and carnivorous CP, we obtained a natural gynogenetic progeny (GBSB). Compared with the maternal parent BSB, GBSB showed different intestinal enzyme activities, microbial composition and transcription profiles of glucose metabolism-related genes. These differences are interrelated and may be affected by paternal fragments. However, metabolomics and functional analysis are needed to determine whether these transcriptional changes are converted into altered metabolic fluxes. Our results provide a relevant framework for understanding the host-microbe-metabolism interactions in gynogenetic fish. However, the mechanisms underlying the changes in the intestinal microbiota under various influences remain unclear and complex, as numerous distinct variation patterns have been reported in existing studies. Further exploration of the specific regulatory mechanisms in the future could provide new insights into the functional mechanisms of the intestinal microbiota in gynogenic fish derived from hybridization between carnivorous and omnivorous fish species, and contribute novel perspectives for the green, efficient, and sustainable development of the aquaculture industry.

Supplementary Information The online version contains supplementary material available at https://doi.org/10.1186/s12864-026-13359-6.

Authors' contributions Ping Wu: Supervision, Writing-original draft, Reviewing, Funding acquisition, Revised manuscript. Yuhuan Wei: Investigation, Validation, Writing-original draft, Reviewing, Revised manuscript. Rui Dai: Investigation, Validation, Writing-original draft, Reviewing.Mingguang Hu: Investigation, Validation, Writing-original draft. Shijia Lei: Investigation, Validation. Jie Tang: Investigation, Validation. Siyao Weng: Data Curation. Yue Ding: Data Curation. Ya Zeng: Formal Analysis. Qinbo Qin: Methodology. Ting Yi: Reviewing. Min Wang: Visualization. Min Tao: Visualization. Chun Zhang: Investigation. Qizhi Liu: Supervision, Reviewing, Funding acquisition, Revised manuscript.. Shaojun Liu: Conceptualization, Supervision, Resources, Reviewing, Funding acquisition.

Funding This research was supported by the National Key R&D Program of China (2022YFD2400601), Yuelushan Laboratory Breeding Program (Grant No. YLS-2025-ZY01011), the National Natural Science Foundation of China (Grant No. U19A2040, 32202919, 32293250, 32293252), the "Xiaohe" Project of Shaoyang. The natural Science Foundation of Hunan Province (Grant No. 2023JJ40434, 2025JJ60871), the science and technology innovation Program of Hunan Province (2022RC1162) and the Special Founds for Construction of Innovative Provinces in Hunan Province (2021NK1010).

Data availability Sequencing data has been deposited in the NCBI Sequence Read Archive (SRA) database (https://dataview.ncbi.nlm.nih.gov/object/PRJNA1303868?reviewer=a4jgu04vrhtndhd55vjp41haqs) under BioProject ID PRJNA1303868 accession numbers SAMN50539832 to SAMN50539840.

Declarations

Ethics approval and consent to participate This study received approval from Institutional Animal Care and Use Committee (IACUC) of Hunan Normal University for all piscine experimental protocols (Permission No. 2025-1009). Fish samples were anesthetized with 100 mg/L MS-222 (Sigma) before dissection.

Consent for publication Not applicable.

Competing interests The authors declare no competing interests.

Open Access This article is licensed under a Creative Commons Attribution-NonCommercial-NoDerivatives 4.0 International License, which permits any non-commercial use, sharing, distribution and reproduction in any medium or format, as long as you give appropriate credit to the original author(s) and the source, provide a link to the Creative Commons licence, and indicate if you modified the licensed material. You do not have permission under this licence to share adapted material derived from this article or parts of it. The images or other third party material in this article are included in the article's Creative Commons licence, unless indicated otherwise in a credit line to the material. If material is not included in the article's

Creative Commons licence and your intended use is not permitted by statutory regulation or exceeds the permitted use, you will need to obtain permission directly from the copyright holder. To view a copy of this licence, visit http://creativecommons.org/licenses/by-nc-nd/4.0/.

References

1. Jiao F, Zhang L, Limbu SM, Yin H, Xie Y, Yang Z, et al. Kong L. Rong HJE, Evolution: A comparison of digestive strategies for fishes with different feeding habits: Digestive enzyme activities, intestinal morphology, and gut microbiota. 2023;13(9):e10499.
2. Li W, Liu J, Tan H, Yang C, Ren L, Liu Q, et al. Zhao RJFim: Genetic effects on the gut microbiota assemblages of hybrid fish from parents with different feeding habits. 2018;9:2972.
3. Austin BJ. The bacterial microflora of fish. Sci World J. 2002;2(1):558–72.
4. Li S, Gu Q, Li Z, Zeng Q, Zhong H, Liu M, et al. The effects of lotus-fish co-culture on the gut microbiome of Hefang crucian carp (*Carassis auratus*). Reprod Breed. 2023;3(3):143–51.
5. Li J, Ni J, Li J, Wang C, Li X, Wu S, et al. Yan QJJoam: Comparative study on gastrointestinal microbiota of eight fish species with different feeding habits. 2014;117(6):1750–60.
6. Escalas A, Auguet J-C, Avouac A, Seguin R, Gradel A, Borrossi L. Villéger SJFiMS: Ecological specialization within a carnivorous fish family is supported by a herbivorous microbiome shaped by a combination of gut traits and specific diet. 2021;8:622883.
7. Daly K, Kelly J, Moran AW, Bristow R, Young IS, Cossins AR. Bravo D. Shirazi-Beechey SPJTJog, microbiology a: Host selectively contributes to shaping intestinal microbiota of carnivorous and omnivorous fish. 2019;65(3):129–36.
8. German DP. Inside the guts of wood-eating catfishes: can they digest wood? J Comp Physiol B. 2009;179(8):1011–23.
9. Clements KD, Angert ER, Montgomery WL, Choat JH. Intestinal microbiota in fishes: what's known and what's not. In.: Wiley Online Library; 2014.
10. Alger EI. Edger PPJCoipb: One subgenome to rule them all: underlying mechanisms of subgenome dominance. 2020;54:108–13.
11. Xu X, Hu E, Xiao Q, Huang X, Wang C, Xu X, et al. Formation and biological characteristics analysis of artificial gynogenetic WuLi carp induced by inactivated sperm of Megalobrama amblycephala. Biology (Basel). 2025;14(8).
12. Ringoe E, Birkbeck TJAr. Intestinal microflora of fish larvae and fry. 1999;30(2).
13. Lin M, Zeng C, Jia X, Zhai S, Li Z. Ma YJJoAM: The composition and structure of the intestinal microflora of Anguilla marmorata at different growth rates: a deep sequencing study. 2019;126(5):1340–52.
14. Su X, Ji D, Yao J, Zou Y, Yan MJF. Comparative analysis of intestinal characteristics of largemouth bass (*Micropterus salmoides*) and intestinal flora with different growth rates. Fishes. 2022;7(2):65.
15. Ismail NA, Ragab SH, Abd ElBaky A, Shoeib AR, Alhosary Y, Fekry DJAoMS. Frequency of Firmicutes and Bacteroidetes in gut microbiota in obese and normal weight Egyptian children and adults. 2011;7(3):501-507.
16. Den Besten G, Van Eunen K, Groen AK, Venema K, Reijngoud D-J, Bakker BMJJolr. The role of short-chain fatty acids in the interplay between diet, gut microbiota, and host energy metabolism. 2013;54(9):2325-2340.
17. Morrison DJ, Preston TJ. Formation of short chain fatty acids by the gut microbiota and their impact on human metabolism. Gut Microbes. 2016;7(3):189–200.
18. Liu X-f, Shao J-h, Liao Y-T, Wang L-N, Jia Y, Dong P-j, Liu Z-z, He D-d, Li C, Zhang XJFii. Regulation of short-chain fatty acids in the immune system. 2023;14:1186892.
19. Yao Y, Cai X, Fei W, Ye Y, Zhao M, Zheng CJ. Crifs, nutrition: The role of short-chain fatty acids in immunity, inflammation and metabolism. 2022;62(1):1-12.
20. Liao A, Zhang S, Yu Q, Wang Y, Tan H, Wu P, et al. Formation and characterization of artificial gynogenetic northern snakehead (Channa argus) induced by inactivated sperm of mandarin fish (Siniperca chuatsi). Aquaculture. 2025;595:741488.
21. Liu Q, Wang S, Tang C, Tao M, Zhang C, Zhou Y, Qin Q, Luo K, Wu C, Hu FJRiA. The research advances in distant hybridization and gynogenesis in fish. 2025;17(1): e12972.
22. Liu Q, Liao A, Tao M, Qin Q, Luo K, Zhang C, et al. Macro-hybrid and micro-hybrid of fish. Rev Aquac. 2025;18(1)
23. Liu S, Wang S, Liu Q, Wu C, Zhou Y, Tao M, et al. The research advances in animal distant hybridization and polyploid organisms. In: Liu S, editor. Fish distant hybridization. Singapore: Springer Nature Singapore; 2022. p. 1–37.
24. Slierendrecht W, Olesen NJ, Juul-Madsen HR, Lorenzen N, Henryon M, Berg P. Søndergaard J. Koch CJF, immunology s: Rainbow trout offspring with different resistance to viral haemorrhagic septicaemia. 2001;11(2):155–67.
25. Wang Y, Liu W, Li Z, Qiu B, Li J, Geng G, et al. Improvement and application of genetic resources of grass carp (Ctenopharyngodon idella). Reproduction and Breeding. 2024;4(3):126–33.
26. Wu Q, Wu Z, Wang L, Lu Y, Bi W, Zhou D, et al. Comparative study on growth performance and morphological characteristics of the meio-and mito-gynogenesis olive flounder (Paralichthys olivaceus). 2021;535:736387.

27. Fu W, Chu X, Xiao W, Shen T, Peng L, Wang Y, et al. Identification of gynogenetic Megalobrama amblycephala induced by red crucian carp sperm and establishment of a new hypoxia tolerance strain. 2022;548:737608.
28. Wang S, Tang C, Tao M, Qin Q, Zhang C, Luo K, et al. Xiao JJSCLS: Establishment and application of distant hybridization technology in fish. 2019;62(1):22–45.
29. Liu S, Wang S, Liu Q, Zhou Y, Zhang C, Tao M, Luo K. The Summary of Fish Distant Hybridization. 2022.
30. Zhang X, Liu F, Bei L, Yu J, Duan L, Huang Z, et al. Comparative analysis of nutrients in muscle and ovary between an improved fish and its parents. Reproduct Breed. 2024;4(1):16–21.
31. Zheng GD, Guo DD, Wu CB, Chen J, Jiang XY, Zou SMJAR. The obvious heterosis and genetic characters of intergeneric cross and backcross juveniles between blunt snout bream (*Megalobrama amblycephala*) and topmouth culter (*Culter alburnus*). Aquac Res. 2019;50(6):1634–43.
32. Mao Z, Fu Y, Wang Y, Wang S, Zhang M, Gao X, et al. Evidence for paternal DNA transmission to gynogenetic grass carp. BMC Genet. 2019;20(1).
33. Calduch-Giner JA, Sitjà-Bobadilla A. Pérez-Sánchez JJFip: Gene expression profiling reveals functional specialization along the intestinal tract of a carnivorous teleostean fish (Dicentrarchus labrax). 2016;7:359.
34. Bonder MJ, Kurilshikov A, Tigchelaar EF, Mujagic Z, Imhann F, Vila AV, et al. Smeekens SPJNg: The effect of host genetics on the gut microbiome. 2016;48(11):1407–12.
35. Wu P, Ji W, Zeng Y, Tang J, Wu C, Qin Q, et al. The analysis of growth performance and expression of growth-related genes in natural gynogenic blunt snout bream muscle derived from the blunt snout bream (Megalobrama amblycephala, ♀) × Chinese perch (Siniperca chuatsi, ♂). Aquaculture. 2024;590.
36. Kaushik SJ, Seiliez I. Protein and amino acid nutrition and metabolism in fish: Current knowledge and future needs. Aquac Res. 2010;41:322–32.
37. Wang Y, Yao J, Liao A, Tan H, Luo Y, Wu P, et al. The formation of hybrid fish derived from hybridization of Megalobrama amblycephala (♀) × Siniperca chuatsi (♂). Aquaculture. 2022;548.
38. Wu P, Zeng Y, Qin Q, Wu C, Wang Y, Zhao R, et al. Comparative analysis of the texture, composition, antioxidant capacity and nutrients of natural gynogenesis blunt snout bream and its parent muscle. Reproduction and Breeding. 2022;2(4):149–55.
39. Huang C, Wu P, Jiang W-D, Liu Y, Zeng Y-Y, Jiang J, et al. Deoxynivalenol decreased the growth performance and impaired intestinal physical barrier in juvenile grass carp (Ctenopharyngodon idella). Fish Shellfish Immunol. 2018;80:376–91.
40. Rao X, Huang X, Zhou Z, Lin X. An improvement of the 2ˆ(-delta delta CT) method for quantitative real-time polymerase chain reaction data analysis. 2013(0976–1594 (Print)).
41. Li W, Liu J, Tan H, Yang C, Ren L, Liu Q, et al. Genetic effects on the gut microbiota assemblages of hybrid fish from parents with different feeding habits. Front Microbiol. 2018;9.
42. Liu S, Wang S, Liu Q, Zhou Y, Zhang C, Tao M, et al. The summary of fish distant hybridization. In: Liu S, editor. Fish distant hybridization. Singapore: Springer Nature Singapore; 2022. p. 325–43.
43. Jiao F, Zhang L, Limbu SM, Yin H, Xie Y, Yang Z, et al. A comparison of digestive strategies for fishes with different feeding habits: digestive enzyme activities, intestinal morphology, and gut microbiota. Ecol Evol. 2023;13(9).
44. Metón I, Mediavilla D, Caseras A, Cantó E, Fernández F, Baanante IV. Effect of diet composition and ration size on key enzyme activities of glycolysis–gluconeogenesis, the pentose phosphate pathway and amino acid metabolism in liver of gilthead sea bream (Sparus aurata). Br J Nutr. 2007;82(3):223–32.
45. Zhang L, Liu C, Jiang Q, Yin Y. Butyrate in Energy Metabolism: There Is Still More to Learn. Trends Endocrinol Metab. 2021;32(3):159–69.
46. Chen P, Zhu Y, Wu X, Gu X, Xue M, Liang X. Metabolic adaptation to high-starch diet in largemouth bass (Micropterus salmoides) was associated with the restoration of metabolic functions via inflammation, bile acid synthesis and energy metabolism. Br J Nutr. 2023;129(3):381–94.
47. Béjà O, Sharpton TJ, Riesenfeld SJ, Kembel SW, Ladau J, O'Dwyer JP, Green JL, Eisen JA, Pollard KS. PhylOTU: A High-Throughput Procedure Quantifies Microbial Community Diversity and Resolves Novel Taxa from Metagenomic Data. PLoS Comput Biol. 2011;7(1).

Publisher's Note Springer Nature remains neutral with regard to jurisdictional claims in published maps and institutional affiliations.

Authors and Affiliations

Yuhuan Wei[1] · Rui Dai[1] · Mingguang Hu[1] · Shijia Lei[1] · Jie Tang[1] · Siyao Weng[1] · Ya Zeng[1] · Yue Ding[1] · Qinbo Qin[1,2,3] · Ting Yi[1] · Min Wang[1,2] · Min Tao[1,2,3] · Chun Zhang[1,2,3] · Ping Wu[1,2] · Qizhi Liu[1,2] · Shaojun Liu[1,2,3]

✉ Ping Wu
wuping@hunnu.edu.cn

✉ Qizhi Liu
lqz@hunnu.edu.cn

✉ Shaojun Liu
lsj@hunnu.edu.cn

[1] State Key Laboratory of Developmental Biology of Freshwater Fish, Engineering Research Center of Polyploid Fish Reproduction and Breeding of the State Education Ministry, College of Life Sciences, Hunan Normal University, Changsha, Hunan 410081, China

[2] Yuelushan Laboratory, Changsha, Hunan 410128, P.R. China

[3] Hunan Yuelu Mountain Scienece and Technology Co.Ltd. for Aquatic Breeding, Changsha, Hunan 410081, China